PROCEEDINGS, Thirty-Seventh Workshop on Geothermal Reservoir Engineering
Stanford University, Stanford, California, January 30 - February 1, 2012
SGP-TR-194

DEEP-SEATED FRACTURES IN HOT GRANITES: A NEW TARGET FOR ENHANCED GEOTHERMAL SYSTEMS?

Christoph E. Schrank[1], Ali Karrech[2], Klaus Regenauer-Lieb[2, 3, 4], Doone Wyborn[5]

1) Queensland University of Technology
QUT Science and Engineering Faculty
GPO Box 2434
Brisbane, QLD, 4001
Australia
e-mail: schrankce@gmail.com
2) CSIRO Earth Science and Resource Engineering
26 Dick Perry Avenue
Kensington, Perth WA 6151
Australia
3) Western Australian Geothermal Centre of Excellence
at the
4) University of Western Australia, School of Earth and Environment
35 Stirling Highway,
Crawley, Perth WA 6009
Australia
5) Geodynamics Limited
Level 3, 19 Lang Parade, PO Box 2046
Milton, QLD 4064
Australia

ABSTRACT

We present finite-element models of interacting brittle and ductile deformation as a method for predicting deep-seated fracture zones developing on time scales of ka to ma (Regenauer-Lieb et al., 2006). These fractures could prove important for the stimulation and extraction of geothermal energy from hot granites. We investigate in particular how deep-seated ductile faults experiencing creep cavitation, emerging from the base of the brittle-ductile transition, propagate upward and interact with brittle faults. Our models use a damage mechanics formulation (Karrech et al., 2011a, b) that considers fractures in the framework of continuum mechanics. Both brittle and creep damage lead to material degradation described by a damage parameter, which in turn is related to energy feedbacks in the model. This approach has been successful in describing seismic behavior in the brittle crust (Lyakhovsky and Ben-Zion, 2008). However, it has been extended only recently (Karrech et al., 2011a) to considering creep damage in the ductile realm.

Creep fractures are microscopic cavities that preferentially develop along grain boundaries during ductile deformation (Cocks and Ashby, 1982). During protracted deformation, they can self-organize into macroscopic failure zones. They are commonly observed in the deformation of high-temperature ceramics and metals (Lemaitre, 1985; Tvergaard, 1982) and are expected to occur in deforming rocks (Regenauer-Lieb, 1999; Rybacki et al., 2008). The creep-cavitation phenomenon was documented just recently in natural hot granites deformed at 400-500°C in the Red Bank shear zone in Central Australia (Fusseis et al., 2009). Here, we model scenarios for fracture propagation in middle and upper continental crust subjected to far-field contraction. Our models predict that brittle fractures are triggered by upward-propagating ductile faults and concentrate near the brittle-ductile transition. These fractures may play a fundamental role in providing fluid pathways in hot rocks. We therefore recommend targeting them specifically for stimulation.

INTRODUCTION

Geothermal heat in hot granitoids is an important potential energy source (Murphy et al., 1985). However, the low permeability of granitic rock poses a significant geotechnical problem for heat extraction. Reservoir stimulation is usually employed for the creation and enhancement of fluid pathways in these rocks. Pre-existing zones of high permeability such as localized large-scale fracture zones may facilitate reservoir stimulation and heat extraction (Batchelor et al., 1987; Evans et al., 1999). Thus, it is desirable to predict the location and geometry of natural fracture zones in hot granitoids. It is expected that many granitoids host fracture zones (Evans et al., 1999). Intrusive rocks have often experienced some form of tectonism at some stage of their history. Moreover, far-field stresses imposed at plate boundaries can lead to the very slow deformation even of continental interiors (with strain rates of order 10^{-17} to 10^{-16} s^{-1}) typically regarded as tectonically inactive (Quigley et al., 2010; Sandiford et al., 2004). Finally, thermal-elastic stresses due to cooling and exhumation commonly induce micro-cracking, jointing, and fracturing (Bruner, 1979, 1984; Engelder, 1985; Engelder et al., 1977; Nadan and Engelder, 2009). Here, we numerically investigate the formation of fracture zones in a deep-seated hot granite body induced by slow contraction.

CONTINUUM-MECHANICAL FRAMEWORK

We employ a novel thermodynamically consistent approach to continuum damage mechanics (Karrech et al., 2011a, b). The approach considers both associated and non-associated elastoviscoplastic materials in the same framework. Therefore, our model allows for brittle and ductile failure. The flow rules and the yield function are derived from Helmholtz free-energy and dissipation functionals using the maximum-entropy production principle, thus permitting thermodynamically consistent material response and deformation localization (Hobbs et al., 2011; Regenauer-Lieb et al., 2010). Material degradation by isotropic damage is considered (Karrech et al., 2011a). Physically, this damage corresponds to the generation of new surfaces (i.e., voids) on the micro-scale, for example due to micro-cracking or creep cavitation. The damage parameter, D, can be regarded as ratio of damaged over undamaged material (Cocks and Ashby, 1980, 1982). Damage leads to a decrease of a material's thermal-elastic properties (Cooper and Simmons, 1977; Saenger et al., 2006; Spatschek et al., 2009) and thus material weakening expressed by the shrinkage of the plastic yield envelope. Our approach is implemented in the finite-element method (Karrech et al., 2011b). A Lagrangian formulation with implicit integration is employed.

MODEL GEOMETRY

We consider a rectangular 2D plane-strain model consisting of 5 layers (Fig. 1). Layers 1 to 3 mimic siliciclastic sedimentary rocks. Layers 4 and 5 correspond to granites with high heat production. Layer 4 has the highest heat production (Table 1). To facilitate fracture localization in the model, we perturbed the surface of layer 4 with a sinusoidal shape of 400 m amplitude and 10 km wavelength. The reference model has a total thickness of 18 km. Model width corresponds to 2.5 wavelengths of the surface perturbation of layer 4 (25 km). We use 4-node bilinear first-order quadrilateral elements with an edge length of 60 m (417 x 300 elements).

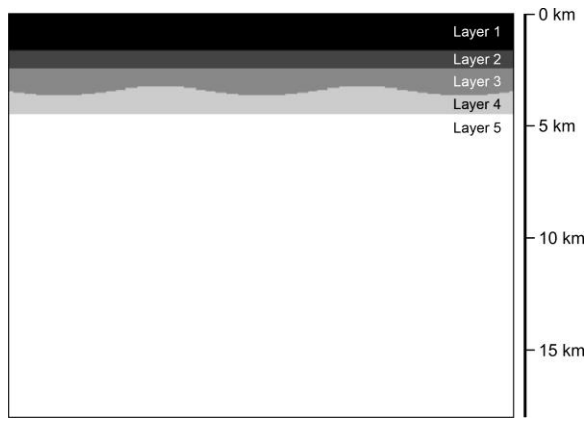

Figure 1: Model geometry

LOADING STEPS AND INITIAL/BOUNDARY CONDITIONS

We apply two sequential loading steps. The first loading steps lasts 1.5 ma and serves to obtain thermal and mechanical equilibrium in the model. Gravity is ramped up linearly to its full value over the first 1.5 ka. Constant temperature boundary conditions are applied to the model surface (0°C) and bottom (500°C). A non-linear temperature field representing a hot geotherm is prescribed at the beginning of the step and equilibrates to a stable field over the equilibration step (Fig. 2). The model surface is free. Nodes at the model bottom can only move in horizontal direction. Nodes at the vertical sides can only move in vertical direction. In the second loading step, a constant horizontal velocity corresponding to a bulk strain rate of 10^{-16} s^{-1} is applied to the left side of the model where nodes can move both in horizontal and vertical direction. The temperature and stress field are inherited from the equilibration step, and so are all boundary conditions except for that of the now moving left side. Step duration is 2.5 ma.

RHEOLOGY

The rheology is serial elastoviscoplasticity with isotropic continuum damage (Karrech et al., 2011a, b). Elasticity is linear, homogeneous, and isotropic. The plastic yield envelope is smooth and described by an exponential function (Karrech et al., 2011b), thus converging to a finite value at infinite depth. We assume that the viscous rheologies of the upper and middle continental crust are controlled by power-law flow and diffusion creep of wet quartz (Bürgmann and Dresen, 2008; Carter and Tsenn, 1987). For power-law flow, we employ laboratory flow laws that bracket the range of existing flow laws (Hirth et al., 2001; Rutter and Brodie, 2004b). To our knowledge, there is only one diffusion-creep law for wet quartz (Rutter and Brodie, 2004a). Elastic and plastic material properties are given in Table 1. The damage parameter is isotropic and hence a scalar. It assumes values between 0 (undamaged) and 0.8 (maximum damage permitted here). Damage nucleation is tied to equivalent plastic strain (Karrech et al., 2011a). Here, damage nucleates if an equivalent plastic strain of 0.5% is exceeded. The constitutive model is derived in detail in (Karrech et al., 2011b).

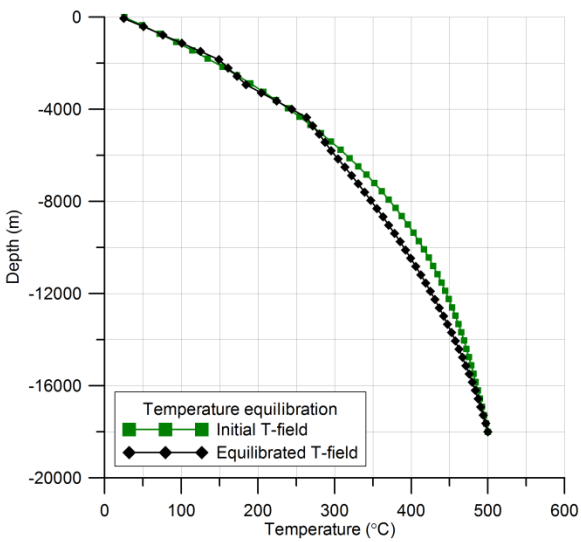

Figure 2: Vertical profiles of initial and equilibrated temperature field.

RESULTS

The evolution, geometry and degree of localization of the modeled fracture system depend on a number of parameters: model geometry, lithological inventory, the constitutive properties of the materials, boundary conditions, and mesh size (in the brittle domain). However, a comprehensive parameter sensitivity study is beyond the scope of this paper. Instead we focus on the impact of the viscous rheology on fracture evolution, which turned out to be of fundamental significance. The choice of viscous rheology controls the thickness and strength of the brittle and ductile part of the crust, respectively (Fig. 3). Therefore, results for two end-member models are presented: a "weak" model with the wet-quartz rheology of Hirth et al. (2001), and a "strong" model with the wet-quartz rheology of Rutter and Brodie (2004b).

The weak model

Fig. 3a displays a map of von Mises' stress (the second invariant of the deviatoric stress tensor) for the weak model after 2.5 ma of shortening. Due to the low strain rate and the hot geotherm, Hirth's et aliorum (2001) flow law predicts a shallow brittle-ductile transition (BDT). Conjugate, relatively gently dipping (30° – 40°) ductile shear zones localize at the bottom of the BDT, which coincides with the inter-face of granite and overlying sediments at about 4 km depth. The tips of these shear zones induce stress concentrations at the bottom of the brittle lid, thus loading it from below. A map of the damage parameter after 2.5 ma of shortening (Fig. 4a) reveals that damage follows these stress concentrations, causing localized brittle failure in the brittle lid (between 3 and 4 km depth). The evolution of the damage parameter is interesting. Fig. 5a shows vertical cross sections of the damage parameter measured in the model center at three different times. A damage wave emerges from model bottom at early stages of the experiment. It travels upward in a diffuse manner, is amplified, and finally localizes as highly damaged brittle-ductile faults at the BDT.

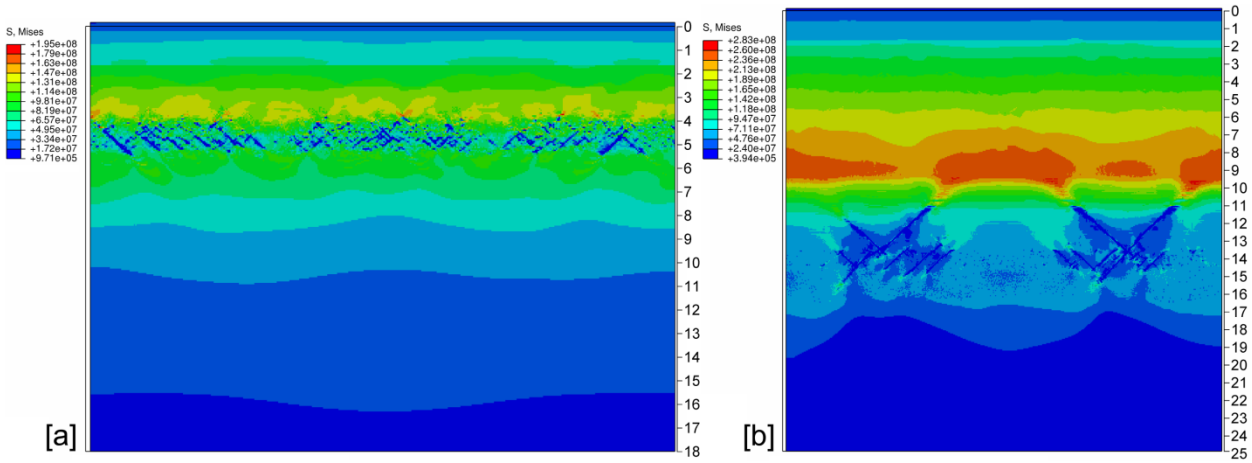

Figure 3: Maps of von Mises' equivalent stress (color scale in Pa) for weak [a] and strong [b] model after 2.5 ma of shortening. Vertical axis denotes depth in km. Superposed black boxes indicate initial model shape.

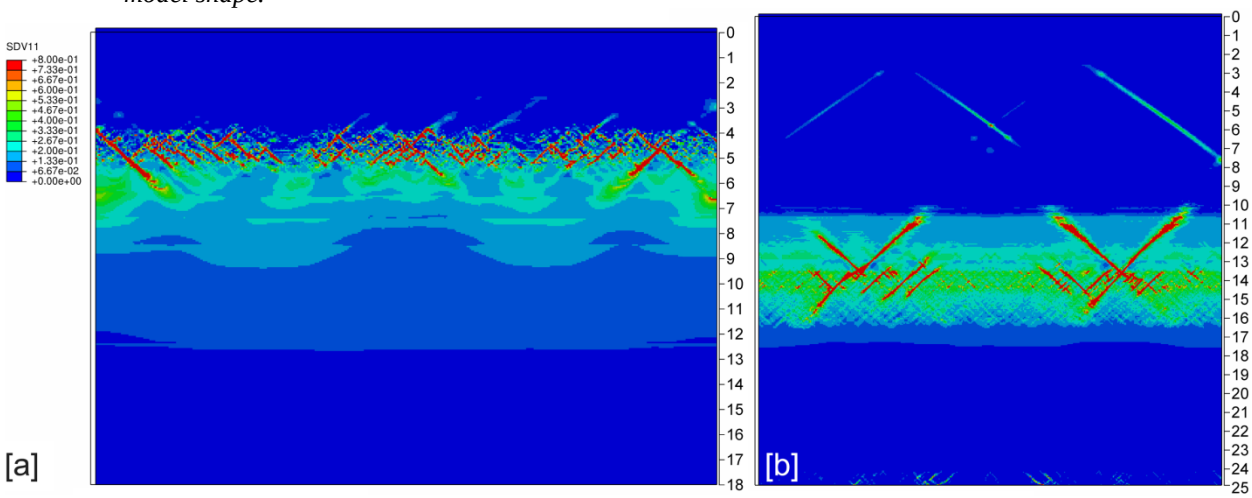

Figure 4: Maps of damage parameter for weak [a] and strong [b] model after 2.5 ma of shortening. Vertical axis denotes depth in km. Superposed black boxes indicate initial model shape.

The strong model

Note that the strong model extends to a depth of 25 km to generate a very weak layer at the model bottom, as in the weak model. In this way, boundary effects are avoided. The temperature at the model bottom is 580°C, thus resulting in the same equilibrated temperature field between 0 and 18 km depth employed in the weak model (Fig. 2). The flow law of Rutter and Brodie (2004b) leads to a markedly thicker and stronger brittle lid (Fig. 3b). The BDT occurs at ~ 10 km depth for the low strain rate and high temperatures employed here. Ductile shear zones localize at the bottom of the BDT and load the brittle lid due to stress concentrations at their tips, as in the weak model. However, these shear zones are steeper (35° – 45°) and do not extend into brittle fault zones, as revealed by a map of the damage parameter (Fig. 4b). In contrast, brittle fault zones develop between 3 and 8 km depth and are not connected to ductile shear zones at the base of the BDT. The general time evolution of the damage parameter is similar to that of the weak model (Fig. 5b): a diffuse damage wave emerges from the model bottom and, after amplification, collapses into highly damaged ductile faults at the bottom of the brittle lid.

DISCUSSION AND CONCLUSION

Our models suggest that the depth of the BDT has a major impact on the location, geometry and rheological nature of fault systems induced by slow contraction of the upper and middle granitic continental crust. If the viscous quartz rheology is weak, as implied by the flow law of Hirth et al. (2001), the BDT is expected to occur at a shallow depth of ~ 4 km in areas of high heat flow. In this case, fairly gently dipping ductile faults form at the base of the BDT as damage collapses into localized structures at this depth. These shear zones load the brittle crust and extend into brittle faults. If the

viscous rheology is strong (Rutter and Brodie, 2004b), the brittle lid is thick, and the BDT occurs at ~ 10 km depth. Highly damaged, steeper ductile faults form at the base of the BDT again. Over the time of our model run, they do not connect with brittle faults formed between 3 and 8 km depth. Protracted deformation might lead to interaction and finally interconnection of brittle and ductile faults in this model. However, we only model fault initiation here. This is because processes such as damage healing, metamorphosis and fluid transport are ignored but will affect fault localization and maintenance of fault systems significantly (Hobbs et al., 2010; Jamtveit et al., 2008; Lyakhovsky and Ben-Zion, 2009; Mancktelow and Pennacchioni, 2004; Neuzil, 2003). Yet fully coupled modeling of thermal, mechanical, chemical, and hydrological processes is still in its infancy and one of the great future challenges in computational geomechanics (Poulet et al., 2009).

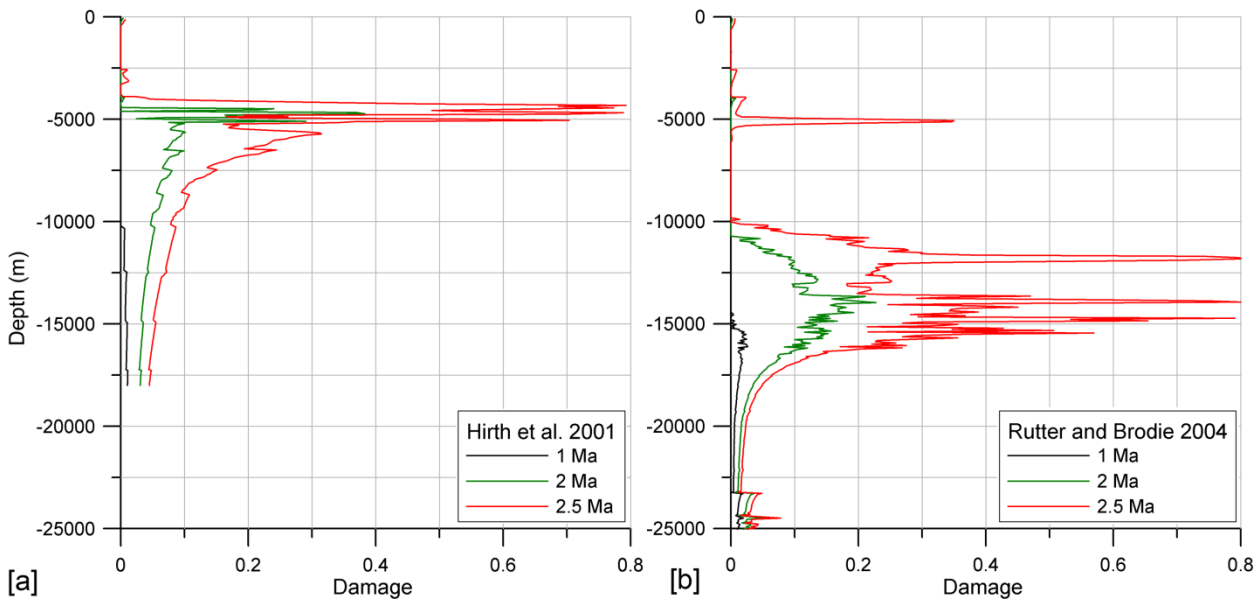

Figure 5: Vertical profiles of damage parameter through model center of weak [a] and strong [b] model at different times (see inset).

Table 1: Material properties

Layer	Young's modulus (Pa)	Poisson's ratio	Density (kg/m^3)	Conductivity ($WK^{-1}m^{-1}$)	Specific heat ($JKg^{-1}K^{-1}$)
1	1.0×10^{10}	0.36	2500	1.15	1250
2	2.5×10^{10}	0.25	2500	2.30	1250
3	4.3×10^{10}	0.25	2550	1.30	1200
4	6.5×10^{10}	0.30	2650	3.00	1000
5	6.5×10^{10}	0.30	2700	2.50	1000
Layer	Expansivity (K^{-1})	Yield stress at zero pressure (MPa)	Yield stress at infinity (MPa)	Heat production (□Wm^{-3})	
1	1.0×10^{-6}	7.81	500	1.0	
2	1.0×10^{-5}	7.81	500	2.0	
3	5.0×10^{-6}	7.81	500	1.0	
4	7.5×10^{-6}	7.81	500	10.0	
5	7.5×10^{-6}	7.81	500	5.0	

In conclusion, both end-member models underline the importance of ductile damage and faulting near the BDT. At its bottom, this rheological interface consistently concentrates ductile deformation and damage emerging from the lower ductile crust.

The plastic-strain wave originating at the model bottom is followed by a diffuse damage wave, which in turn facilitates ductile deformation. Although fluid transport is not modeled here, it is conceivable that this damage wave may serve as a diffuse carrier of fluids from the lower crust which then are concentrated in shear zones at the BDT (Fusseis et al., 2009).

This makes pre-existing fracture systems in hot granites an interesting target for enhanced geothermal systems. They do not only provide zones of enhanced permeability but may be connected to deeper brittle-ductile faults that tap into fluid and heat reservoirs below the BDT.

ACKNOWLEDGEMENTS

C. Schrank is grateful for funding by the German Research Foundation (DFG) under grant no. SCHR 1262/1-1. This work was supported by the Western Australian State Government through the Premier's Fellowship, the Western Australian Geothermal Centre of Excellence Program, and Geodynamics Ltd.

REFERENCES

Batchelor, A. S., Kwakwa, K., and Garnish, J. D., 1987, Stimulation and flow processes in hot dry rock reservoirs: Geothermics, v. 16, no. 4, p. 447-449.

Bruner, W. M., 1979, Crack growth and the thermoelastic behavior of rocks: Journal of Geophysical Research, v. 84, no. B10, p. 5578-5590.

-, 1984, Crack growth during unroofing of crustal rocks: effects on thermoelastic behavior and near-surface stresses: Journal of Geophysical Research, v. 89, no. B6, p. 4167-4184.

Bürgmann, R., and Dresen, G., 2008, Rheology of the lower crust and upper mantle: Evidence from rock mechanics, geodesy, and field observations, Annual Review of Earth and Planetary Sciences, Volume 36, p. 531-567.

Carter, N. L., and Tsenn, M. C., 1987, Flow properties of continental lithosphere: Tectonophysics, v. 136, no. 1-2, p. 27-63.

Cocks, A. C. F., and Ashby, M. F., 1980, Intergranular fracture during power-law creep under multiaxial stresses: Metal science, v. 14, no. 8-9, p. 395-402.

-, 1982, On creep fracture by void growth: Progress in Materials Science, v. 27, no. 3-4, p. 189-244.

Cooper, H. W., and Simmons, G., 1977, The effect of cracks on the thermal expansion of rocks: Earth and Planetary Science Letters, v. 36, no. 3, p. 404-412.

Engelder, T., 1985, Loading paths to joint propagation during a tectonic cycle: an example from the Appalachian Plateau, U.S.A: Journal of Structural Geology, v. 7, no. 3-4, p. 459-476.

Engelder, T., Sbar, M. L., and Kranz, R., 1977, A mechanism for strain relaxation of barre granite: Opening of microfractures: Pure and Applied Geophysics, v. 115, no. 1, p. 27-40.

Evans, K. F., Cornet, F. H., Hashida, T., Hayashi, K., Ito, T., Matsuki, K., and Wallroth, T., 1999, Stress and rock mechanics issues of relevance to HDR/HWR engineered geothermal systems: review of developments during the past 15 years: Geothermics, v. 28, no. 4–5, p. 455-474.

Fusseis, F., Regenauer-Lieb, K., Liu, J., Hough, R. M., and De Carlo, F., 2009, Creep cavitation can establish a dynamic granular fluid pump in ductile shear zones: Nature, v. 459, no. 7249, p. 974-977.

Hirth, G., Teyssier, C., and Dunlap, J., 2001, An evaluation of quartzite flow laws based on comparisons between experimentally and naturally deformed rocks: International Journal of Earth Sciences, v. 90, no. 1, p. 77-87.

Hobbs, B. E., Ord, A., and Regenauer-Lieb, K., 2011, The thermodynamics of deformed metamorphic rocks: A review: Journal of Structural Geology, v. 33, no. 5, p. 758-818.

Hobbs, B. E., Ord, A., Spalla, M. I., Gosso, G., and Zucali, M., 2010, The interaction of deformation and metamorphic reactions: Geological Society, London, Special Publications, v. 332, no. 1, p. 189-223.

Jamtveit, B., Malthe-Sørenssen, A., and Kostenko, O., 2008, Reaction enhanced permeability during retrogressive metamorphism: Earth and Planetary Science Letters, v. 267, no. 3-4, p. 620-627.

Karrech, A., Regenauer-Lieb, K., and Poulet, T., 2011a, Continuum damage mechanics for the lithosphere: J. Geophys. Res., v. 116, no. B4, p. B04205.

-, 2011b, A damaged visco-plasticity model for pressure and temperature sensitive geomaterials: International Journal of

Engineering Science, v. 49, no. 10, p. 1141-1150.

Lemaitre, J., 1985, A continuous damage mechanics model for ductile fracture: Journal of Engineering Materials and Technology, v. 107, p. 83-89.

Lyakhovsky, V., and Ben-Zion, Y., 2008, Scaling relations of earthquakes and aseismic deformation in a damage rheology model: Geophysical Journal International, v. 172, no. 2, p. 651-662.

-, 2009, Evolving geometrical and material properties of fault zones in a damage rheology model: Geochem. Geophys. Geosyst., v. 10, no. 11, p. Q11011.

Mancktelow, N. S., and Pennacchioni, G., 2004, The influence of grain boundary fluids on the microstructure of quartz-feldspar mylonites: Journal of Structural Geology, v. 26, no. 1, p. 47-69.

Murphy, H., Drake, R., Tester, J., and Zyvoloski, G., 1985, Economics of a conceptual 75 MW hot dry rock geothermal electric power-station: Geothermics, v. 14, no. 2–3, p. 459-474.

Nadan, B. J., and Engelder, T., 2009, Microcracks in New England granitoids: A record of thermoelastic relaxation during exhumation of intracontinental crust: Geological Society of America Bulletin, v. 121, no. 1-2, p. 80-99.

Neuzil, C. E., 2003, Hydromechanical coupling in geologic processes: Hydrogeology Journal, v. 11, no. 1, p. 41-83.

Poulet, T., Regenauer-Lieb, K., and Karrech, A., 2009, A unified multi-scale thermodynamical framework for coupling geomechanical and chemical simulations: Tectonophysics, v. 483, no. 1-2, p. 178-189.

Quigley, M. C., Clark, D., and Sandiford, M., 2010, Tectonic geomorphology of Australia: Geological Society, London, Special Publications, v. 346, no. 1, p. 243-265.

Regenauer-Lieb, K., 1999, Dilatant plasticity applied to Alpine collision: Ductile void growth in the intraplate area beneath the Eifel volcanic field: Journal of Geodynamics, v. 27, no. 1, p. 1-21.

Regenauer-Lieb, K., Karrech, A., Chua, H. T., Horowitz, F. G., and Yuen, D., 2010, Time-dependent, irreversible entropy production and geodynamics: Philosophical Transactions of the Royal Society A: Mathematical, Physical and Engineering Sciences, v. 368, no. 1910, p. 285-300.

Regenauer-Lieb, K., Weinberg, R. F., and Rosenbaum, G., 2006, The effect of energy feedbacks on continental strength: Nature, v. 442, no. 7098, p. 67-70.

Rutter, E. H., and Brodie, K. H., 2004a, Experimental grain size-sensitive flow of hot-pressed Brazilian quartz aggregates: Journal of Structural Geology, v. 26, no. 11, p. 2011-2023.

-, 2004b, Experimental intracrystalline plastic flow in hot-pressed synthetic quartzite prepared from Brazilian quartz crystals: Journal of Structural Geology, v. 26, no. 2, p. 259-270.

Rybacki, E., Wirth, R., and Dresen, G., 2008, High-strain creep of feldspar rocks: Implications for cavitation and ductile failure in the lower crust: Geophysical Research Letters, v. 35, no. 4.

Saenger, E., Krüger, O., and Shapiro, S., 2006, Effective Elastic Properties of Fractured Rocks: Dynamic vs. Static Considerations: International Journal of Fracture, v. 139, no. 3, p. 569-576.

Sandiford, M., Wallace, M., and Coblentz, D., 2004, Origin of the in situ stress field in south-eastern Australia: Basin Research, v. 16, no. 3, p. 325-338.

Spatschek, R., Gugenberger, C., and Brener, E. A., 2009, Effective elastic moduli in solids with high density of cracks: Physical Review B, v. 80, no. 14, p. 144106.

Tvergaard, V., 1982, Ductile fracture by cavity nucleation between larger voids: Journal of the Mechanics and Physics of Solids, v. 30, no. 4, p. 265-286.